

Microelectronic thin film deposition by ultraviolet laser photolysis

F. K. Boyer, C. A. Moore, R. Solanki,* W. K. Ritchie,† G. A. Roche,** G. J. Collins
Department of Electrical Engineering, Colorado State University, Fort Collins, Colorado 80523

Abstract

An excimer laser is used to photochemically deposit thin films of silicon dioxide, silicon nitride, aluminum oxide, and zinc oxide at low temperatures (100-350°C). Deposition rates in excess of 3000 Å/min and conformal coverage over vertical walled steps were demonstrated. The films exhibit low defect density and high breakdown voltage and have been characterized using IR spectrophotometry, AES, and C-V analysis. Device compatibility has been studied by using photodeposited films as interlayer dielectrics, diffusion masks, and passivation layers in production CMOS devices.

Additionally, we have deposited metallic films of Al, Mo, W, and Cr over large (>5 cm²) areas using UV photodissociation of trimethylaluminum and the refractory metal hexacarbonyls. Both shiny metallic films as well as black particulate films were obtained depending on the deposition geometry. The black films are shown to grow in columnar grains. The depositions were made at room temperature over pyrex and quartz plates as well as silicon wafers. We have examined the resistivity, adhesion, stress and step coverage of these films. The films exhibited resistivities at most ~20 times that of the bulk materials and tensile stress no higher than 7×10^8 dynes/cm².

Introduction

There exists a need for low-temperature semiconductor fabrication processes to minimize wafer warpage, dopant redistribution, and defect generation and propagation.¹ Moreover, film deposition over photoresist for applications such as tri-level resists for high-resolution lithography and direct patterning via lift-off is desired at temperatures below ~200°C (above which resist degradation occurs).² In this work we discuss a new low temperature, high deposition rate (up to 5000 Å/min) film growth technique which uses an excimer laser to photolyze gas-phase reactants whose products condense and form the desired film. This technique has been used to deposit dielectric films of SiO₂, Si₃N₄, Al₂O₃ and ZnO, and conducting films of Al, Cr, Mo, and W. The properties of these films are reviewed and compared to conventional deposition techniques.

Experimental Apparatus

A Lumonics 860T excimer laser provides ultraviolet photons in a beam of rectangular cross-section which is down-collimated to a cross-sectional area of 12 x 1.5 mm for parallel deposition, as shown in Figure 1, or is expanded using a negative lens to deposit over large

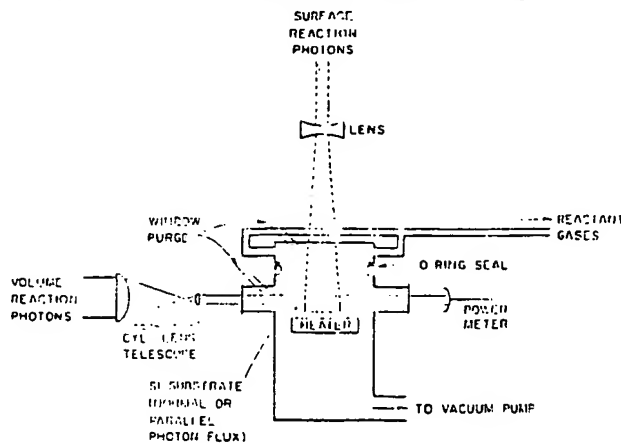


Figure 1. Experimental Set-Up.

†NCR Microelectronics, Fort Collins, CO 80526

*Present Address: Johns Hopkins University, Dept. of Physics, Baltimore, MD 21218.

**Present Address: Thermco Inc., Orange, CA 92668.

BEST AVAILABLE COPY

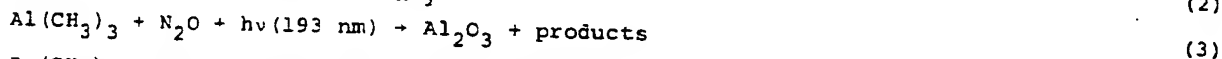
areas during normal irradiation. The insulating films in this work were deposited using a wavelength of 193 nm (ArF* transition) while the metallic films were deposited using either 193 nm or the 248 nm (KrF*) wavelength; repetition rate for each wavelength was 90-100 Hz. UV transmitting windows were purged with a rare gas to prevent deposition on them. Surface reaction photons, whose role is described herein, were provided by a low pressure mercury lamp or by folding back the portion of the beam transmitted through the cell. A substrate heater capable of heating up to 500°C was used during the deposition of dielectric films.

A major advantage of this experimental scheme is the ability to vary laser power, wavelength, and spatial location independently while not affecting the deposition process. This is in direct contrast to plasma-enhanced CVD where process parameters are strongly inter-related and one is limited to pressure regimes where a discharge can be started and maintained. The only pressure constraint on the laser CVD technique is that the gases used for a given deposition must be at optically thin concentrations. Thus beam attenuation across a sample is minimized and thickness uniformity is preserved. For example, deposition of SiO₂ is possible at total pressures up to 8 torr since the beam intensity will vary by less than 10% across a 3 inch wafer at this pressure.

Additionally, conformal step coverage is possible by this technique due to the photo-dissociation volume being an "infinite plane source" with respect to topographical features on the sample. This is demonstrated herein.

Deposition of Oxide and Nitride Films

Films of SiO₂, Si_xN_y, Al₂O₃ and ZnO have been deposited via the following reactions, respectively:



The silicon-compound insulator films are compared to the competitive low-temperature deposition schemes of plasma-enhanced and mercury photosensitized CVD, while the metal oxides are discussed on the basis of their properties alone.

Typical deposition conditions for deposition of SiO₂ are shown in Table 1a. A relatively

Table 1. Typical Deposition Conditions

		RF Plasma ¹		Hg Photox ^{TM,3}	
a) SiO ₂	Laser	380°C		100-200°C	
Substrate temperature	150-400°C	1.1 Torr		0.3-1 Torr	
Cell pressure	6 Torr	33		25	
N ₂ O/SiH ₄	73	300 Å/min		120 Å/min	
Deposition rate	600 Å/min (He buffer) 800 Å/min (N ₂ buffer)				
b) Si _x N _y	Laser	RF Plasma ¹		Hg Photride ^{TM,3}	
Substrate temperature	200-425°C	380°C		150-200°C	
Cell pressure	2 Torr	2 Torr		4 Torr	
NH ₃ /SiH ₄	1	7		30	
	10 SCCM NH ₃ 10 SCCM SiH ₄ 50 SCCM N ₂				
Deposition rate	700 Å/min	350 Å/min		65 Å/min	
c) Al ₂ O ₃	Laser	RF Planar Magnetron ²			
Substrate temperature	100-400°C	150-400°C			
Cell pressure	1 Torr	10 ⁻² Torr			
Deposition rate	1500 Å/min (up to 1 μ/min)	350 Å/min			

¹Reactor manufactured by ASM, Phoenix, AZ.

²R. S. Nowicki, J. Vac. Sci. Tech. 14(1), 127 (1977).

³Tylan Corporation, Solid State Technology, Dec. 1982.

high reactant gas ratio N₂O/SiH₄ was used in this work. Deposition rates (which are for films of area ~20 cm²) could be increased using a higher silane density since this reactant is optically transparent at 193 nm. Deposition rates of ~5000 Å/min have been observed over areas of ~3 cm².

BEST AVAILABLE COPY

The electrical, chemical and physical properties of the laser CVD SiO_2 films have been measured. The films are comparable to plasma and photo-sensitized CVD films with respect to adhesion, stress, index of refraction, stoichiometry, and hydrogen incorporation as shown in Table 2. The laser deposited films are inferior compared to plasma-enhanced CVD films in

Table 2. Comparison of Deposited SiO_2 Films

	Laser CVD	Plasma	Hg Photox
Breakdown voltage (MV/cm)	6.5-8 (1000 Å film)	10 (2000 Å)	4-8 (1000-10,000 Å)
Resistivity ($\Omega\text{-cm}$) at 5 MV/cm	up to 6.7×10^{13}	10^{16}	2×10^{12}
Stoichiometry	SiO_2	SiO_2	$\text{SiO}_{1.9}$
H content (by IR)			
as Si-H (at.%)	1-4	<4	None
as Si-OH (at.%)	<1	<1	None
Etch Rate in 5:1 BHF	>55	22 (7:1 BHF)	140
Refractive index	1.48	1.49	1.46
Stress on Si (10^9 dyne/cm ²) (all compressive)	1.5	3.6	2

terms of electrical resistivity (~ 100 times lower), dielectric strength (20% lower breakdown voltage), and etch rate in a buffered oxide etch ($\sim 2 \times$ faster). Laser CVD films exhibited the lowest internal stress and pinhole densities. A 1000 Å SiO_2 film photodeposited at 400°C had no pinholes in 5 cm², while a 2000 Å plasma CVD film showed $<1/\text{cm}^2$ and a 10,000 Å photox SiO_2 film had 5 to 10 per square centimeter. In the laser CVD approach conformal step coverage is achieved over a wide range of deposition conditions. Figure 2 shows SiO_2

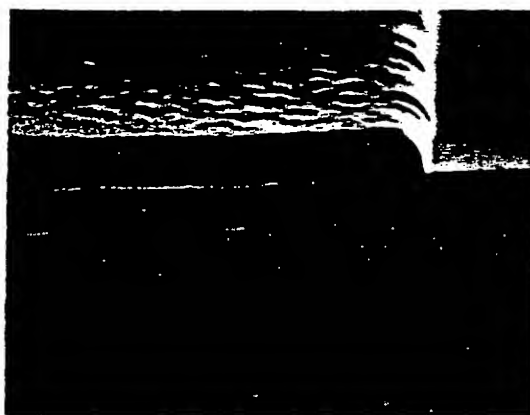


Figure 2. Step Coverage of SiO_2 Over 4000 Å Polysilicon Step.

(~ 5000 Å thick) photodeposited over a 4000 Å polysilicon step which was formed on an oxidized silicon wafer. It should be noted the rough surface atop the step is due to the underlying poly-Si while the even morphology of the oxide is retained below the step, over smooth oxidized Si wafer.

Silicon nitride has also been deposited using laser-induced CVD using the reaction equation (2). The conditions for deposition are similar to the two techniques under comparison and to those of the SiO_2 deposition process discussed above (Table 1b). A notable difference is that lower concentrations of ammonia are required since its absorption cross-section is $\sim 10^3$ higher than nitrous oxide at 193 nm.³ Deposition rate is still much higher than that of plasma or mercury sensitized reactions.

Again the photodeposited films have comparable physical properties (i.e. adhesion, compressive stress, refractive index, step coverage and stoichiometry) as shown in Table 3. Pinhole densities are comparable to plasma CVD films but superior to photride films. The laser CVD films lack in terms of etch rates; they etch approximately ten times faster than plasma deposited nitrides. However, at the bottom of Table 3 the effect of low level surface irradiation can be seen. As deposited at 380°C, the laser CVD silicon nitride films etched at 44 Å/sec in 5:1 buffered oxide etch, indicative of a porous or low density film. Illumination during deposition with 254 nm photons from a low pressure mercury discharge lamp reduced this etch rate to 27 Å/sec. This etch rate was reduced further to 8 Å/sec by folding

BEST AVAILABLE COPY

Table 3. Comparison of Deposited Silicon Nitride Films

	Laser CVD <SiN	Plasma >SiN	Hg Photronic Variable
Stoichiometry			
Impurities (at. %)			
H by IR-as Si-H	12	12-16	-----
as N-H	11-20	2-7	<"typical plasma"
O by ESCA	<5	-----	-----
Etch rate (Å/sec)	15 (dep. at 425°C)	1.7	12
in 5:1 BOE		(7:1 BOE)	
No surface photons	44 (dep. at 380°C)	-----	-----
254 nm photons	27	-----	-----
193 nm photons	8	-----	-----

back the transmitted portion of the 193 nm dissociating laser beam. The power density of both on the substrate surface was weak so as to not cause surface heating. Clearly, a surface reaction is occurring but has not been modeled at this time. Refer to Fig. 1 for surface photon irradiation geometry.

Using this technique, oxides of aluminum and zinc have been deposited but are not as fully characterized at this time. Conditions for Al_2O_3 growth are tabulated in Table 1c. As compared to films obtained by RF plasma deposition, the laser CVD Al_2O_3 films show comparable adhesion, stress, stoichiometry, and refractive index. As with the silicon compound discussed previously, the photodeposited films show higher etch rate ($\times 10$) but have a low pinhole density (none in 5 cm^2 for an 1100 Å laser CVD film versus $36/\text{cm}^2$ for a 2500 Å plasma deposited film). The only other major difference known presently is that the photodeposited films have shown up to 1% carbon contamination, probably due to dissociation of methyls in the aluminum donor gas. The effect of this impurity on the electrical properties is not known at this time.

To obtain ZnO, an oxygen donor, either NO_2 or N_2O was introduced into the cell together with dimethylzinc (DMZ). At 248 nm laser wavelength (KrF) and using N_2O as the oxygen donor, clear films of ZnO were obtained but at a very slow deposition rate ($\sim 200 \text{ Å/min}$). There was a slight increase in the deposition rate at 193 nm . The results at 248 nm with NO_2 were not any better. The highest deposition rate (5000 Å/min) was obtained with NO_2 irradiated at 193 nm . Best results with respect to both the deposition rate and stoichiometry of the films were obtained with NO_2 flow rate of 34 sccm and DMZ pressure of 30 mTorr . The He window purge flow rate was 100 sccm . An automatic throttling valve maintained the total cell pressure at 2 Torr . The substrate temperatures ranged from room temperature to a maximum of 220°C .

The deposited ZnO films appeared clear. Uniform films over $2 \text{ cm} \times 5 \text{ cm}$ area were obtained at deposition rates of over 5000 Å/min . The difference in thickness over 5 cm (end to end) was less than 5%. It should be pointed out that the uniformity of the deposited ZnO films is important for fabrication of surface acoustic wave (SAW) devices. At higher deposition rates ($\sim 1 \mu/\text{min}$) the films had a tendency to peel when exposed to atmospheric pressure and were nonuniform.

The stoichiometry of the deposited film, by ESCA, showed the films to be composed of 49% Zn and 51% oxygen. Carbon was less than 1% and there was no measureable trace of N. By increasing the ratios of DMZ to NO_2 flows, ZnO stoichiometry was easily changed causing the measured sheet resistivities to range from 10^3 to $10^{-1} \text{ ohms/square}$ for 0.5μ thick films. The refractive index of the stoichiometric film, deposited at 200°C was measured on an ellipsometer to be 1.86. The index of refraction increased with the abundance of Zn in the film and with higher deposition temperatures as expected.

When the film adhesion was measured, in all cases the Si substrates cracked ($\sim 10^9 \text{ dynes/cm}^2$) before the ZnO films could be detached. The stress of the photodeposited ZnO film was determined by the x-ray technique. The stress of a 2000 Å thick ZnO film on a Si wafer was $7 \times 10^9 \text{ dynes/cm}^2$ tensile. The etch rate in 5:1 buffered oxide etch (BOE) of ZnO deposited at 200°C was found to be $< 20 \text{ Å/min}$. The pinhole density of 1000 Å thick film of ZnO deposited at 180°C was measured on a Gasonics pinhole monitor to be $< 1 \text{ cm}^2$.

Deposition of Metals

We have previously reported laser-induced deposition of refractory metals over small areas (10^{-4} cm^2).⁵ As an extension of our earlier work we have investigated large area ($> 5 \text{ cm}^2$) photodeposition of Al, Mo, W and Cr. Uniform films of these metals were deposited on pyrex and quartz substrates as well as silicon wafers at room temperature. We have examined the resistivity, adhesion, stress, and step coverage of these films.

Plasma assisted CVD of refractory metals occurs as low as 350°C (nm/min deposition rates) for refractory halides⁶ but plasma parameters such as rf power and frequency, gas flow,

electrode spacing, total pressure and substrate heating are all interrelated and difficult to control individually. Photodissociation occurs only along the path of the laser beam, unlike plasma excitation, therefore there is less impurity generation from the walls due to plasma ion bombardment. Moreover, the cracking pattern is less complex in photodissociation and hence we have better control and repeatability of deposition conditions.

Our experimental arrangement is shown in Figure 1. All substrates were precleaned in HF and deionized water prior to deposition. The substrates were held either parallel or normal to the incident laser beam. Either a reservoir containing the carbonyl or a flask of trimethylaluminum (TMA) was connected to the cell. For the carbonyls, both the reservoir and the pyrex connecting tube were heated with a heater tape to about 50°C.

The substrate was first placed into its holder and the cell pumped down with a roughing pump to a few microns. The laser then irradiated the substrate to preclean the surface with the UV radiation; this improves the adhesion of the deposited films. The vacuum pump was then throttled to reduce the cell throughput and the donor gas introduced into the cell. The deposited films appeared as bright silvery films. When the beam was parallel to the substrate, black particulate films of columnar growth resulted, as shown in Figure 3. For

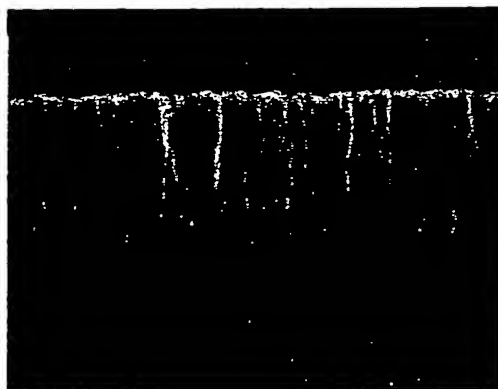


Figure 3. Columnar Grain Growth of Chromium Film. Magnification is 20,000X.

this reason, all the films characterized were obtained at normal incidence. Thick ($>1 \mu$) Cr and Mo films deposited at room temperature had a tendency to peel when exposed to air. This could be avoided by heating the substrate to about 150°C during deposition or prior to removal from the cell. All the photodeposited films discussed below were obtained at room temperature.

The purity of photodeposited films was examined by Auger and ESCA analysis. The major impurity in all the films was oxygen ($<7\%$) probably due to the relatively poor vacuum obtained with a roughing pump. We hope to reduce this impurity by using a improved deposition cell and a better vacuum system. A surprising result was the relatively low concentration of carbon in these films (Table 4). The most carbon-free films and the highest deposition

Table 4. Summary of the Physical Properties of the Laser Deposited Al, Mo, W and Cr Films

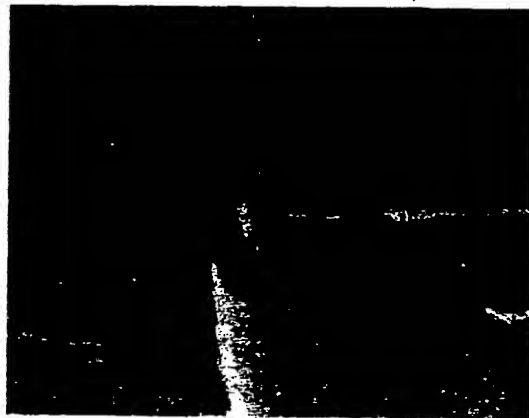
	Deposition Rate (Å/min)	Resistivity ($\mu\Omega$ -cm)		Percent Carbon in Film	Adhesion, on quartz (dynes/cm ²)	Tensile Stress (dynes/cm ²)
		bulk	film			
Mo	2500	5.2	36	<0.9	$>5.5 \times 10^8$	$<3 \times 10^9$
W	1700	5.65	135	<0.7	$>6.5 \times 10^8$	$<2 \times 10^9$
Cr	2000	12.9	210	<0.8	$>5.4 \times 10^8$	$<7 \times 10^9$
Al	1000	2.66	3.0	<4.0	$>5.5 \times 10^8$	$<1 \times 10^9$

rates were obtained using a laser wavelength of 248 nm; 0.25, 0.17, 0.10 and 0.2 μ /min deposition rates were measured for Mo, W, Al and Cr, respectively, over 2.5 x 2.5 cm area. But even this low contamination by carbon can limit the obtainable film resistivity.⁷ These rates will vary with the laser power, the cell pressure, and the size of the area over which the film is deposited. The film over the 2.5 x 2.5 cm area was uniform to $\pm 15\%$. It should be pointed out that the area of deposition can be varied by changing the divergence of the laser beam with a lens; with tight focusing and substrate or beam translation, patterned lines can be deposited.

The adhesion of the photodeposited films was measured. In the case of W, the machine reached its upper limit without detaching the films, while in the case of Al, Mo and Cr, the quartz substrates chipped off before the films were detached. Of the four metals, Cr films were the least adhesive while W were the best, which remained intact even when placed in an ultrasonic cleaner. The most adhesive films were deposited using the 193 nm laser wavelength for photodissociation. The reasons for the change of carbon content and adhesion with the laser wavelength are not fully understood at this time. Stress measurements of the photodeposited films were made by the substrate bending technique. The metal films were deposited on microscope cover slips and the bowing caused by the films was measured. All the films had tensile stress and none was higher than 7×10^9 dynes/cm²; aluminum showed the lowest amount of stress (1×10^9 dynes/cm²).

The electrical resistivities of the deposited metal films were measured with a four-point probe. These resistivities are tabulated along with the bulk values in Table 4. These resistivities are at most about a factor of 20 higher than bulk resistivity values, while the aluminum had, even with its high carbon content, a resistivity approaching the bulk value.

One important quality of a film deposition technique is the ability of the deposited film to cover vertical-walled steps. Step coverage patterns used to check our deposited refractory films were the same as those used to examine SiO₂ step coverage. The photo-deposited refractory metal thicknesses were varied between 0.2 and 0.6 μ . After deposition, the metal coated wafers were chilled in liquid nitrogen and then cleaved. The step coverage was examined with a SEM. An ~ 5000 Å Al film is shown in Figure 4. It can be seen that the



BEST AVAILABLE COPY

Figure 4. Step Coverage of 5000 Å Aluminum Film Over 4000 Å Polysilicon Step.

film is of even thickness over the flat, as well as the vertical walls, and clearly demonstrates conformal step coverage. The vertical striations in the films are due to wafer cleaving. It is interesting to note that SEM examination of all our films showed absence of microstructures similar to those seen in laser photodeposited Cd and Zn films.⁸

Summary

We have described a technique to deposit oxide, nitride, and metal films via ultraviolet photolysis of gas-phase donor molecules. All films are deposited at fast rates (up to 5000 Å/min) and demonstrate conformal step coverage over vertical steps. The insulating films exhibit low pinhole densities but are inferior in terms of etch rate and electrical resistivity. Surface photon impingement during film deposition is shown to drastically reduce silicon nitride etch rate. Future work will focus in this area. Metallic films have been deposited and exhibit good physical properties. The refractory metals show high resistivities which may be limited by carbon incorporation. The effect of annealing these films has not been studied yet.

Acknowledgements

The authors would like to acknowledge the Office of Naval Research for support of this work.

References

1. S. Su, Solid State Technology 24, 72 (1981).
2. M. P. Lepselter and W. T. Lynch, in VLSI Electronics Microstructure Science, edited by N. G. Einspruch (Academic, New York, 1981) p. 87.

3. J. Zavelovich, M. Rothschild, W. Gornik, and C. K. Rhodes, J. Chem. Phys. 74(12), 15 June 1981, and M. Ashford, M. T. Macpherson, and J. F. Simons, in Topics in Current Chemistry, Vol. 86, (Springer-Verlag, Berlin, 1979) p. 22.
4. J. E. Bowers, R. L. Thornton, B. T. Khuri-Yakub, R. L. Junemian, and G.S. Kino, Appl. Phys. Lett. 41, 805 (1982).
5. R. Solanki, P. K. Boyer, J. E. Mahan, and G. J. Collins, Appl. Phys. Lett. 38, 572 (1981).
6. J. K. Chu, C. C. Tang, and D. W. Hess, Appl. Phys. Lett. 41, 75 (1982).
7. L. H. Kaplan and F. M. D'Heurle, J. Electrochem. Soc. 117, 693, (1970).
8. R. M. Osgood and D. J. Ehrlich, Opt. Lett. 7, 385 (1982).

BEST AVAILABLE COPY

Proceedings of SPIE—The International Society for Optical Engineering

Volume 385

Laser Processing of Semiconductor Devices

Charles C. Tang
Chairman/Editor

Cooperating Organization
Materials Research Society

January 18-19, 1983
Los Angeles, California

BEST AVAILABLE COPY

Published by

SPIE—The International Society for Optical Engineering
P.O. Box 10, Bellingham, Washington 98227-0010 USA
Telephone 206/676-3290 (Pacific Time) • Telex 46-7053

SPIE (The Society of Photo-Optical Instrumentation Engineers) is a nonprofit society dedicated to advancing engineering and scientific applications of optical, electro-optical, and photo-electronic instrumentation, systems, and technology.

86 12XSU 3922
XL
3/05 31150-57

BEST AVAILABLE COPY

LASER PROCESSING OF SEMICONDUCTOR DEVICES

Volume 385

Contents

Conference Committee	iv
Introduction	v
SESSION 1. LASER ANNEALING AND GETTERING	1
385-02 Recent advances in laser processing of semiconductors, A. Kestenbaum, Western Electric Co.	2
385-03 Novel laser scanning techniques for Si-on-insulator devices, L. E. Trimble, G. K. Celler, Bell Labs.	8
385-04 Laser applications to semiconductor device processing, R. R. Shah, Texas Instruments, Inc.	16
385-05 Some new laser processing applications in microelectronics, D. L. Parker, Texas A&M Univ.	24
385-06 Gas immersion laser diffusion (GILDing), R. J. Pressley, XMR, Inc.	30
385-07 Laser activated flow for integrated circuit fabrication, M. Delfino, Fairchild Advanced Research and Development Lab.	32
385-08 Melt depth and regrowth kinetics in pulsed laser annealing of silicon and gallium arsenide, G. J. Galvin, M. O. Thompson, J. W. Mayer, Cornell Univ.; P. S. Peercy, Sandia National Labs.; R. B. Hammond, Los Alamos National Lab.	38
SESSION 2. THREE-DIMENSIONAL INTEGRATION	45
385-09 Circuit simulation of three-dimensional metal oxide semiconductor field effect transistor (MOSFET) device structures in beam-recrystallized polysilicon films, J. F. Gibbons, M. D. Giles, K. F. Lee, J. T. Walker, Stanford Univ.	46
385-10 Conduction processes in polysilicon: effects of laser restructuring, A. N. Khondker, Rice Univ.; R. R. Shah, Texas Instruments; D. M. Kim, Rice Univ.	50
385-12 Electronic properties of grain boundaries in polycrystalline silicon, E. S. Yang, E. Poon, H. L. Evans, W. Hwang, J. S. Song, C. M. Wu, Columbia Univ.	59
385-13 Effects of grain boundaries on channel conduction in thin film polysilicon on silicon-dioxide metal oxide semiconductor field effect transistors (SOI MOSFETs), J. G. Fossum, A. Ortiz, H.-K. Lim, H.-W. Lam, Univ. of Florida	65
385-28 High-performance thin film transistors in CO ₂ laser crystallized silicon on quartz, A. Chiang, W. P. Meuli, N. M. Johnson, M. H. Zarzycki, Xerox Palo Alto Research Ctrs.	76
SESSION 3. LASER PROGRAMMATION AND REDUNDANCY	81
385-15 Characterization of laser blown molydisilicide links, S. Wills, J. McPherson, Texas Instruments Inc.	82
385-17 Laser microsurgery and fabrication of integrated circuits, J. R. Moulic, Y. C. Kiang, R. W. Lang, J. C. Logue, IBM Corp.	87
385-18 Laser redundancy: past, present, and future, E. J. Swenson, Electro Scientific Industries, Inc.	93
385-19 Laser targeting considerations in redundant memory repair, D. Smart, R. Reilly, B. Wells, Teradyne, Inc.	97
385-20 Precision laser irradiation system, E. G. Arthurs, K.-C. Liu, Quantronix Corp.	102
SESSION 4. LASER ETCHING, DEPOSITION, AND LITHOGRAPHY	111
385-21 Laser microchemistry for direct writing of microstructures, R. M. Osgood, Jr., Columbia Univ.; D. J. Ehrlich, T. F. Deutsch, D. J. Silversmith, A. Sanchez, M.I.T.	112
385-23 Maskless laser plating techniques for microelectronic materials, R. J. von Gutfeld, M. H. Gelchinski, L. T. Romankiw, IBM T. J. Watson Research Lab.	118
385-22 Microelectronic thin film deposition by ultraviolet laser photolysis, P. K. Boyer, C. A. Moore, R. Solanki, W. K. Ritchie, G. A. Roche, G. J. Collins, Colorado State Univ.	120
385-25 Rapid laser-induced chemical etching of semiconductors, F. A. Houle, IBM Research Lab.	127
385-24 Laser chemical etching method for drilling vias in GaAs, A. W. Tucker, M. Birnbaum, The Aerospace Corp.	131
385-26 Laser plasma x-ray source optimization for lithography, H. M. Epstein, P. J. Mallozzi, B. E. Campbell, Battelle's Columbus Labs.	141
385-27 Laser-based studies of chemical vapor deposition, W. G. Breiland, M. E. Coltrin, P. Ho, Sandia National Labs.	146
Addendum	152
Author Index	153
Subject Index	154

THIS PAGE BLANK (USPTO)